

Data-driven Reconstruction of the Late-time Cosmic Acceleration with $f(T)$ Gravity

Xin Ren,^{1,2,3,*} Thomas Hong Tsun Wong,^{4,†} Yi-Fu Cai,^{1,2,3,‡} and Emmanuel N. Saridakis^{5,1,2,§}

¹*Department of Astronomy, School of Physical Sciences,*

University of Science and Technology of China, Hefei, Anhui 230026, China

²*CAS Key Laboratory for Research in Galaxies and Cosmology,*

University of Science and Technology of China, Hefei, Anhui 230026, China

³*School of Astronomy and Space Science, University of Science and Technology of China, Hefei, Anhui 230026, China*

⁴*Department of Physics, Faculty of Science, The University of Hong Kong, Pokfulam Road, Hong Kong, China*

⁵*National Observatory of Athens, Lofos Nymfon, 11852 Athens, Greece*

We use a combination of observational data in order to reconstruct the free function of $f(T)$ gravity in a model-independent manner. Starting from the data-driven determined dark-energy equation-of-state parameter we are able to reconstruct the $f(T)$ form. The obtained function is consistent with the standard Λ CDM cosmology within 1σ confidence level, however the best-fit value experiences oscillatory features. We parametrise it with a sinusoidal function with only one extra parameter comparing to Λ CDM paradigm, which is a small oscillatory deviation from it, close to the best-fit curve, and inside the 1σ reconstructed region. Similar oscillatory dark-energy scenarios are known to be in good agreement with observational data, nevertheless this is the first time that such a behavior is proposed for $f(T)$ gravity. Finally, since the reconstruction procedure is completely model-independent, the obtained data-driven reconstructed $f(T)$ form could release the tensions between Λ CDM estimations and local measurements, such as the H_0 and σ_8 ones.

PACS numbers: 98.80.-k, 95.36.+x, 04.50.Kd

I. INTRODUCTION

The concept of dark energy was introduced to explain the acceleration of the expansion of the universe that was discovered in the late 1990s [1, 2]. One of the dark energy candidates is the cosmological constant, leading to the standard cosmological scenario, namely the Λ CDM paradigm. However, as more and more accurate astronomical data accumulate we could deduce that the standard cosmological model might present some undesirable features. Especially, the tensions that seem to appear in the standard cosmological model parameters derived from different observations, if not resulting from unknown systematics, pose a great challenge to modern cosmology. One of the most significant tensions is the tension of Hubble constant. In particular, the direct measurements by Hubble Space Telescope give $H_0 = 74.03 \pm 1.42 \text{ km s}^{-1} \text{ Mpc}^{-1}$ [3], while the Planck 2018 best fit for Cosmic Microwave Background (CMB) data based on Λ CDM paradigm gives $H_0 = 67.4 \pm 0.5 \text{ km s}^{-1} \text{ Mpc}^{-1}$ [4, 5]. The tension between the two observations has reached 4.4σ . Another tension that seems to appear is the so-called σ_8 one, which occurs in the measurement of perturbations of large-scale structures and CMB [6–8]. In principle, one could follow two main ways to solve these tensions. One is to modify the early evolution of the universe to obtain a relatively small sound horizon at the end of drag epoch [9]. The other is to modify the

late evolution of the universe by replacing the cosmological constant with a dynamic dark energy model such as various scalar-field dark energy models [10–13] and modified theories of gravity [14–16]. In the same lines, since the physical nature of dark energy remains unknown until today, physicists have put forward many dynamical dark energy theories too and have constructed various specific scenarios.

In order to determine whether the proposed theories can explain observations, an efficient method is to reconstruct the expression of the unknown function that usually appears in a specific model, from current cosmological observations [6, 17–19]. Recent progress on revealing the dark-energy equation-of-state (EoS) parameter as the function of the redshift has paved the way for the reconstruction of the specific dynamical dark energy models [20, 21]. Especially, the revealed evolution of EoS displays the crossing of the -1 divide. Similarly, other studies with observational constraints on w CDM and $w(z)$ have also shown the possibility that $w < -1$ [22–26], and in particular that the dark-energy EoS parameter may be negative at high redshifts. Such a behavior might be difficult to be explained using a single scalar field or fluid dark energy models [27], and thus inspires us to seek for the modified gravity theory.

One of the most successful theories of gravitational modification is $f(T)$ gravity [15]. In contrast to the curvature scalar R of the standard general relativity, the expression of the torsion scalar T in the cosmological background does not contain the time derivative of the Hubble parameter H . This feature offers a significant advantage in the reconstruction procedure of $f(T)$ comparing to $f(R)$ gravity, and moreover it has the potential to explain the accelerating expansion by using a simple La-

* rx76@mail.ustc.edu.cn

† twht@connect.hku.hk

‡ Corresponding author: yifucui@ustc.edu.cn

§ msaridak@phys.uoa.gr

grangian form. $f(T)$ gravity could alleviate both the H_0 and σ_8 tensions from the perspective of effective field theory [28, 29]. Finally, the constraints on the specific $f(T)$ scenarios due to cosmological observations have been analyzed in detail in [30–34].

In this work we are interested in using combined observational data-sets in order to reconstruct the $f(T)$ function. The structure of the manuscript is as follows: We briefly review $f(T)$ gravity in the context of cosmology in Section II. In Section III we illustrate the observational data sources that we use, and we reconstruct the $f(T)$ function in a model-independent way. Then we propose an analytic $f(T)$ form that can describe it. Finally, we summarize our results and we provide a discussion in Section IV.

II. $f(T)$ GRAVITY AND COSMOLOGY

In this section, we provide a brief review on $f(T)$ gravity and its application in cosmology. The dynamical variables in $f(T)$ gravity are the tetrad fields $e^A{}_\mu$, where Greek indices correspond to the spacetime coordinates and Latin indices correspond to the tangent space coordinates. At each point of the spacetime manifold, the tetrad fields $e^A{}_\mu$ form an orthonormal basis in the tangent space, which implies that they satisfy the relation $g_{\mu\nu} = \eta_{AB} e^A{}_\mu e^B{}_\nu$, with $g_{\mu\nu}$ the spacetime metric and where $\eta_{AB} = (1, -1, -1, -1)$ is the tangent-space metric. We mention here that in order to acquire a covariant formulation of $f(T)$ gravity one needs to consider the spin connection too [35]. However, in the flat Friedmann-Robertson-Walker metric considered in this work one could apply vanishing spin connection, and hence we proceed with the form of pure tetrad teleparallel gravity [35, 36].

We consider the Weitzenböck connection, defined as

$$\hat{\Gamma}^\lambda{}_{\mu\nu} \equiv e_A{}^\lambda \partial_\nu e^A{}_\mu = -e^A{}_\mu \partial_\nu e_A{}^\lambda. \quad (1)$$

For this connection, the Riemann curvature vanishes and we only have non-zero torsion, namely

$$T^\lambda{}_{\mu\nu} \equiv \hat{\Gamma}^\lambda{}_{\nu\mu} - \hat{\Gamma}^\lambda{}_{\mu\nu} = e_A{}^\lambda (\partial_\mu e^A{}_\nu - \partial_\nu e^A{}_\mu). \quad (2)$$

Additionally, the torsion scalar is

$$T = S_\rho{}^{\mu\nu} T^\rho{}_{\mu\nu}, \quad (3)$$

where

$$S_\rho{}^{\mu\nu} \equiv \frac{1}{2} (K^{\mu\nu}{}_\rho + \delta_\rho^\mu T^{\alpha\nu}{}_\alpha - \delta_\rho^\nu T^{\alpha\mu}{}_\alpha) \quad (4)$$

with

$$K^\rho{}_{\mu\nu} \equiv \frac{1}{2} (T_\mu{}^\rho{}_\nu + T_\nu{}^\rho{}_\mu - T^\rho{}_{\mu\nu}). \quad (5)$$

The simplest theory that one can construct in this framework is the teleparallel gravity, whose Lagrangian

is the torsion scalar T . This theory is equivalent to general relativity at the level of equations of motion, since there exists a transformation relation between the torsion scalar T and the curvature scalar R [37–39]. Similarly to $f(R)$ gravity that generalizes the Lagrangian to an arbitrary function of the curvature scalar R , one could also generalize the Lagrangian of teleparallel gravity to an arbitrary function of the torsion scalar T , which is no longer equivalent to its curvature counterpart. Specifically, the generalized Lagrangian could be written as

$$S = \int d^4x e \frac{M_P^2}{2} [T + f(T) + L_m], \quad (6)$$

where $e = \det(e^A{}_\mu) = \sqrt{-g}$, M_P is the Planck mass and $f(T)$ is the arbitrary function of torsion scalar T (we use units where $c = 1$). By varying the above action with respect to the tetrads, we obtain the field equations as

$$\begin{aligned} & e^{-1} \partial_\nu (e e_A{}^\rho S_\rho{}^{\mu\nu}) [1 + f_T] - e_A{}^\lambda T^\rho{}_{\nu\lambda} S_\rho{}^{\nu\mu} [1 + f_T] \\ & + e_A{}^\rho S_\rho{}^{\mu\nu} (\partial_\nu T) f_{TT} + \frac{1}{4} e_A{}^\mu [T + f(T)] \\ & = 4\pi G e_A{}^\rho T(m)_\rho{}^\mu, \end{aligned} \quad (7)$$

where $f_T \equiv \partial g / \partial T$, $f_{TT} \equiv \partial^2 g / \partial T^2$, and $T(m)_\rho{}^\mu$ is the matter energy-momentum tensor.

Concerning the background geometry of the universe we consider the flat Friedmann-Robertson-Walker (FRW) metric, which has the form

$$ds^2 = dt^2 - a^2(t) \delta_{ij} dx^i dx^j, \quad (8)$$

where $a(t)$ is the scale factor. The expression of the torsion scalar under this metric is $T = -6H^2$. Therefore, one advantage of the $f(T)$ gravity is that the torsion scalar T does not contain the time-derivative of the Hubble parameter $H = \dot{a}/a$, which implies that a specific form of $f(T)$ function would connect to the specific phenomenological behaviors in an easy way. Inserting the cosmological metric to the field equations (7) we result to the two modified Friedmann equations as [15]:

$$H^2 = \frac{8\pi G}{3} \rho_m - \frac{f(T)}{6} + \frac{T f_T}{3} \quad (9)$$

$$\dot{H} = -\frac{4\pi G (\rho_m + p_m)}{1 + f_T + 2T f_{TT}}. \quad (10)$$

Comparing these two equations with the standard Friedmann equations with the dark energy component, one obtains the effective energy density and pressure of dark energy as

$$\rho_{f(T)} = \frac{M_P^2}{2} [2T f_T - f(T)] \quad (11)$$

$$p_{f(T)} = \frac{M_P^2}{2} \left[\frac{f(T) - T f_T + 2T^2 f_{TT}}{1 + f_T + 2T f_{TT}} \right]. \quad (12)$$

Finally, the effective EoS parameter of dark energy is defined as

$$w \equiv \frac{p_{f(T)}}{\rho_{f(T)}} = \frac{f(T) - T f_T + 2T^2 f_{TT}}{[1 + f_T + 2T f_{TT}] [2T f_T - f(T)]}. \quad (13)$$

III. DATA-DRIVEN RECONSTRUCTION OF $f(T)$ FUNCTION

In this section we will present a procedure to reconstruct the involved $f(T)$ function using various datasets. In particular, according to the modified Friedmann equations (9), (10), we can associate a specific $f(T)$ form with the observed data through the Hubble parameter. The Hubble parameter can be obtained from the observational data as a function of the redshift, i.e. $H(z)$ [40–42]. By using these data, we can find the relation between the redshift z and f , namely $f(z)$. Then we can substitute the expression of $T(z)$ as a function of z into this relation, resulting to the reconstruction of the specific form of $f(T)$.

In order to follow the above procedure, we need to first extract the expressions for the involved derivatives f_T . Since in the variation of the redshift in the observation data δz is small, we can make the following approximation:

$$f_T \equiv \frac{df(T)}{dT} = \frac{df/dz}{dT/dz} = \frac{f'}{T'}$$

$$f'(z) \approx \frac{f(z + \Delta z) - f(z)}{\Delta z}. \quad (14)$$

Hence, the modified Friedmann equation (9), assuming dust matter (i.e. $p_m = 0$), can be written as

$$H^2(z) = H_0^2 \left[(1 - \Omega_M) \frac{\rho_{f(T)}(z)}{\rho_{f(T)}(0)} + \Omega_M (1 + z)^3 \right]. \quad (15)$$

Now, using Eq. (14) we can extract the recursive relation between the consecutive redshifts (z_i and z_{i+1}), namely

$$f(z_{i+1}) - f(z_i) = 3(z_{i+1} - z_i) \frac{T'(z_i)}{T(z_i)} \cdot \left[H^2(z_i) - \frac{8\pi G}{3} \rho_m(z_i) + \frac{f(z_i)}{6} \right]. \quad (16)$$

By inserting the expressions of the function $T(z)$, $H(z)$ and $\rho_m(z)$ into the above equation, it can be transformed into

$$f(z_{i+1}) = f(z_i) + 6(z_{i+1} - z_i) \frac{H'(z_i)}{H(z_i)} \cdot \left[H^2(z_i) - H_0^2 \Omega_{m0} (1 + z_i)^3 + \frac{f(z_i)}{6} \right]. \quad (17)$$

In summary, we deduce that we could reconstruct the evolution of $f(z)$ in $f(T)$ cosmology, using the $H(z)$ data. Specifically, if we have the values of H and f at a given redshift z_i , the value of f at the next redshift z_{i+1} would be totally determined. Finally, concerning the initial conditions, they can be determined by using the observational values at $z = 0$.

A. Numerical Reconstruction

In this subsection we proceed to the specific application of the above procedure. Observing (15) we deduce that in order to calculate the evolution of f we need to insert the values of $w(z)$ reconstructed by the data. This $w(z)$ was reconstructed in [20] through a combination of observational data called ALL16, where a Bayesian, non-parametric procedure using the Monte Carlo Markov Chain method was performed. These data-sets ALL16 include the Planck 2015 [43], the JLA supernovae [44], the 6dFRS [45] and SDSS main galaxy sample BAO measurements [46], the WiggleZ galaxy power spectra [47], weak lensing from CFHTLenS [48], local measurements of Cepheids [49], $H(z)$ measurements [50], BAO and RSD measurements [51] and Ly α BAO measurements [6]. We are interested in the reconstruction results of the first 29 bins corresponding to redshift z between 0 and 2.3 shown in Fig. 1.

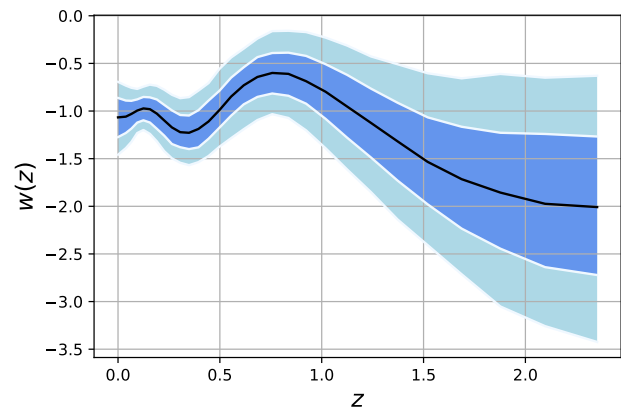


FIG. 1. The data-driven reconstructed $w(z)$ of [20]. The dark and light blue correspond to 1σ and 2σ confidence levels respectively, while the black curve denotes the best-fit value.

Hence, we can now plug the value of $w(z)$ to each bin and use the modified Friedmann equation (15) to solve for the effective energy density and the Hubble parameter. The high-redshift bins solution are depended on the low redshift solution through [52]:

$$H^2(z) = H_0^2 \left[(1 - \Omega_M) \frac{\rho_{f(T)}(z)}{\rho_{f(T)}(0)} + \Omega_M (1 + z)^3 \right], \quad (18)$$

where the $\rho_{f(T)}(z)$ can be represented in terms of w_j , for z in bin j , as

$$\rho_{f(T)}(z) = \rho_{f(T)} \Big|_{z=0} \left(\frac{1+z}{1+z_j - \Delta z_j/2} \right)^{3(1+w_j)} \times \prod_{i=1}^{j-1} \left(\frac{1+z_i + \Delta z_i/2}{1+z_i - \Delta z_i/2} \right)^{3(1+w_i)}. \quad (19)$$

Additionally, a set of $H(z)$ and $H'(z)$ can be solved for each sample through the Friedmann equation (15), and

then a set of reconstructed $f(z)$ can be obtained using equation (17). Generating the $w(z)$ samples repeatedly with $w(z)$ mean data and covariance matrix between the different bins, we can obtain the corresponding distribution of $H(z)$, $H'(z)$ and $f(z)$. Then we can acquire the sample distribution range of 1σ and 2σ confidence level, as well as the best-fit (mean).

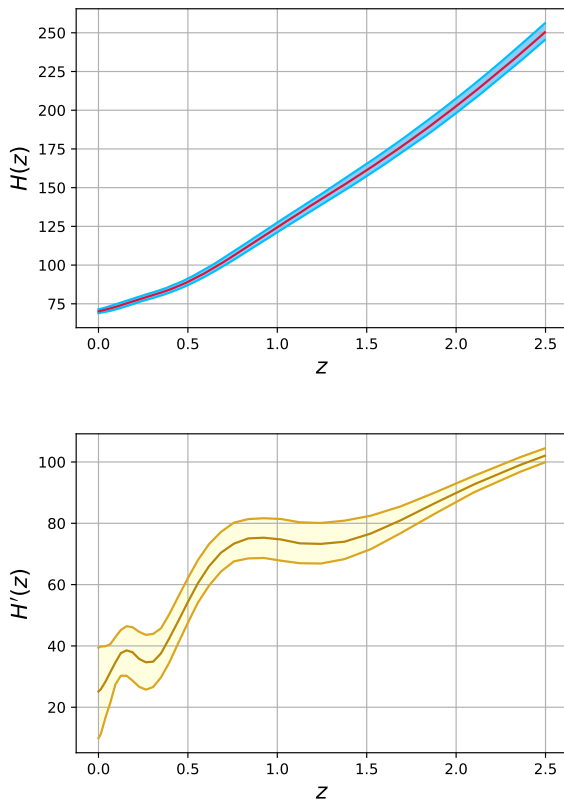


FIG. 2. The reconstructed behavior of $H(z)$ (upper graph) and $H'(z)$ (lower graph), arising from the data-driven reconstructed $w(z)$ of Fig. 1, with the present-day values $H_0 = 70.2 \pm 1.3 \text{ km s}^{-1} \text{ Mpc}^{-1}$ and $\Omega_{m0} = 0.289$. In both graphs, the dark curves denote the best fit, while the shaded area marks the allowed region at 1σ confidence level.

The best-fit curve, as well as the 1σ range, of $H(z)$ and $H'(z)$ are shown in Fig. 2. Here we choose the present-day values $H_0 = 70.2 \pm 1.3 \text{ km s}^{-1} \text{ Mpc}^{-1}$ and $\Omega_{m0} = 0.289$ [20] as boundary condition to reconstruct the evolution history. Furthermore, the $H'(0)$ can be obtained from the sample of $w(0)$ and H_0 , and the equation (9).

Having reconstructed $H(z)$ and $H'(z)$, we can now proceed to the reconstruction of $f(z)$ distribution using relation (17). In Fig. 3 we present the corresponding best-fit curve, as well as the 1σ and 2σ regions, for the reconstructed $f(z)$. Now, as mentioned above, knowing $f(z)$ and using the relation between the torsion scalar and the Hubble parameter, namely $T = -6H(z)^2$, it is trivial to convert $f(z)$ to $f(T)$. Hence, in Fig. 4 we present the

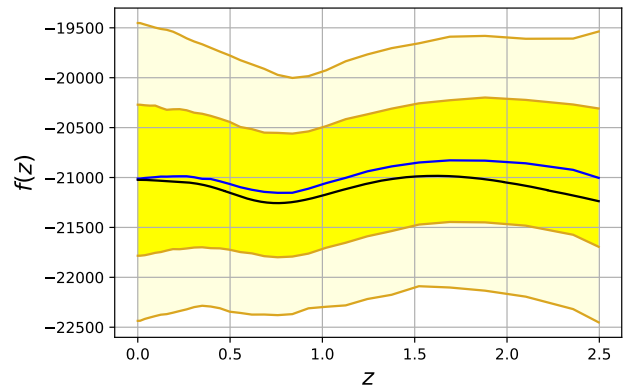


FIG. 3. The reconstructed behavior for $f(z)$ as a function of redshift z , arising from the data-driven reconstructed $H(z)$ and $H'(z)$ of Fig. 2. The yellow and light yellow regions mark the 1σ and 2σ confidence level respectively, the blue curve represents the reconstructed mean values, and the black curve arises using the best-fit curve of $w(z)$ of Fig. 1.

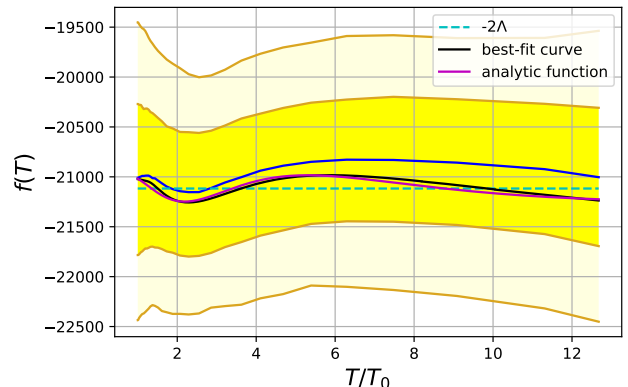


FIG. 4. The reconstructed $f(T)$ form, arising from the data-driven reconstructed $f(z)$ of Fig. 3. The yellow and light yellow regions mark the 1σ and 2σ confidence level respectively, the blue curve represents the reconstructed mean values, and the black curve arises using the best-fit curve of $f(z)$ of Fig. 3. Finally, the magenta curve is the analytical function given in Eq. (20).

reconstructed $f(T)$ as a function of T , where we mention that the units of both T and $f(T)$ are $(\text{km s}^{-1} \text{ Mpc}^{-1})^2$. We mention that we have not assumed any ansatz form for $f(T)$ or any prior for the involved parameters, on the contrary the reconstruction of f is entirely model-independent, and based solely on observational data. This $f(T)$ reconstruction is the main result of the present work.

We close this section by making some comments on the reconstruction procedure based on the Gaussian processes approach [53, 54]. Such processes can get a set of random variables in which any finite number of variables is subject to a joint normal distribution. Gaussian processes are fully defined by their mathematical expect-

tations and kernel functions. The expectation and kernel functions can be obtained from known data. Hence, with the help of Gaussian Processes in Python (GAPP) we can reconstruct the evolution of functions and their derivatives from the given data points [54]. Since the dark-energy EoS is constant inside each bin, the entire $w(z)$ is not continuous. Under the condition that $H(z)$ solved in different bin is continuous, perfect continuity cannot be guaranteed for $H'(z)$. In order to guarantee the continuity of $H'(z)$, the idea of Gaussian process is considered. Indeed, we use GAPP to reconstruct the $H(z)$ and $H'(z)$ from the $H(z)$ obtained from the solution of the modified Friedmann equation shown above. This method can avoid the discontinuity among different bins and improve the continuity of $H(z)$ and $H'(z)$. The Gaussian processes details are presented in Appendix A.

B. Analytical results

In this section we proceed by investigating the possible analytic form of the data-driven reconstructed $f(T)$ function. Observing the graph of the reconstructed $f(T)$ function, a first conclusion is that the constant form $f(T) = -2\Lambda$, which corresponds to the cosmological constant and thus to Λ CDM cosmology, lies within the 1σ region. This is a cross-check verification of our analysis, and it is in agreement with the results of other reconstructed procedures [40, 42].

The best-fit for the $f(T)$ function is close to the constant one, nevertheless it presents a slight oscillatory behavior which in turn is capable of describing the oscillatory behavior of the dark-energy EoS parameter arising from the simultaneous consideration of various observational data-sets (see Fig. 1). The sinusoidal function is a good choice for characterizing oscillations. In this case, we need at least three parameters to describe the amplitude, frequency and phase of the oscillation. Observing the detailed form of the best-fit curve of Fig. 4, we conclude that we can fit it very efficiently with a function of the form

$$f(T) = \alpha T_0 \sin\left(\frac{\beta}{T/T_0 + \delta} - \gamma\right) - 2\Lambda, \quad (20)$$

with $T_0 = -6H_0^2$, namely a varying sinusoidal function for the oscillation (the first term in (20)) and the rightmost boundary condition owing to its tight constraint (the second term in (20)). Note that the parameters $\alpha, \beta, \delta, \gamma$ are dimensionless while Λ has the units of T . Hence, the above $f(T)$ form is a small oscillatory deviation from the Λ CDM cosmology. In particular, the exact confrontation of the numerically obtained best-fit curve with the above analytical form gives $\alpha T_0 = 132 \text{ (km s}^{-1}\text{Mpc}^{-1})^2$, $\beta = 47.1$, $\delta = 3.27$, $\gamma = 161$, $\Lambda = 10558 \text{ (km s}^{-1}\text{Mpc}^{-1})^2$, while the maximum deviation of our best-fit empirical formula from the numerical data in y -axis is ≈ 23.8 , which is well within the 1σ regime.

Nevertheless, note that the analytical expression (20) is the one that matches the numerically reconstructed best-fit $f(T)$ form perfectly. One can definitely use an oscillatory function with less free parameters that will still be close to the best-fit curve of Fig. 4 and deep inside the 1σ regime. This could be

$$f(T) = \alpha T_0 \sin\left(\frac{T_0}{T}\right) - 2\Lambda, \quad (21)$$

which still is a small oscillatory deviation from Λ CDM cosmology with only one extra free parameter (for $\alpha = 0$ Λ CDM cosmology is recovered), and thus with significantly improve information criteria values, such as the Akaike Information Criterion (AIC), the Bayesian Information Criterion (BIC), and the Deviance Information Criterion [33]. We mention that similar oscillatory dark-energy scenarios are known to be in good agreement with the observational data [55–60], however up to our knowledge this is the first time that such a behavior is proposed for $f(T)$ modified gravity.

IV. CONCLUSIONS

In this work we used a combination of observational data in order to reconstruct the $f(T)$ function of $f(T)$ modified gravity in a model-independent manner. Starting from the data-driven reconstructed dark-energy EoS parameter of [20], we first reconstructed both $H(z)$ and $H'(z)$ using two methods: the modified Friedmann equations approximation and the Gaussian processes. In particular, since the original $w(z)$ data is divided into bins, in order to ensure that $H(z)$ is continuous between consecutive bins, from the differential equation solution we obtain a slightly discontinuous $H'(z)$. Thus, application of the Gaussian processes provided a continuous reconstructed $H'(z)$, however the reconstruction results for $f(T)$ form present an increase uncertainty of the function distribution, which is more significant at higher redshift boundary. Comparing the two methods, we found that using Friedmann equations can guarantee the correlation of $H(z)$ and $H'(z)$. Hence, overall, this approach can lead to very efficient constraints on the reconstruction result.

From the reconstructed $H(z)$ and $H'(z)$ we were able to reconstruct $f(z)$ and finally $f(T)$. The obtained data-driven reconstructed function is consistent with the standard Λ CDM cosmology within 1σ confidence level. However, the best-fit value of the reconstructed model has obvious characteristics of oscillatory evolution. In order to describe these features we parametrized it with an oscillatory, sinusoidal, function, with four free parameters that indeed leads to a perfect fit. Inspired by this, we then proposed an oscillatory, sinusoidal function with only one extra parameter comparing to Λ CDM paradigm, which still is a small oscillatory deviation from it, close to the best-fit curve, and definitely inside the 1σ reconstructed region. Similar oscillatory dark-energy scenarios

are known to be in good agreement with observational data, nevertheless this is the first time that such a behavior is proposed for $f(T)$ gravity. Finally, since the proposed model has only one extra free parameter, it is expected to lead to very good information criteria values.

The reconstruction procedure followed above is completely model-independent, especially Λ CDM-independent, and it is based solely on a collection of intermediate-redshift and low-redshift data-sets. Hence, we expect that the obtained data-driven reconstructed $f(T)$ model could release the tensions between Λ CDM estimations and local measurements, such as the H_0 and σ_8 ones. Definitely, a detailed and direct confrontation of the proposed oscillatory function with the data should be performed before we can consider it as a successful modified gravity candidate. Such an analysis lies beyond the scope of the present work and it is left for a future project.

ACKNOWLEDGMENTS

We thank Chunlong Li, Martiros Khurshudyan, Yuting Wang, and Gongbo Zhao for extensive discussions. This work is supported in part by the NSFC (Nos. 11653002, 11961131007, 11722327, 1201101448, 11421303), by the CAST-YESS (2016QNR001), by the National Youth Talents Program of China, by the Fundamental Research Funds for Central Universities, by the CSC Innovation Talent Funds, and by the USTC Fellowship for International Cooperation. All numerical calculations were operated on the computer clusters *LINDA* & *JUDY* in the particle cosmology group at USTC.

Appendix A: Gaussian Process approach

The Gaussian process is a stochastic procedure in order to obtain a collection of random variables, namely to acquire a reconstruction function directly from the known data [53, 54]. The data determine the covariance (kernel) function through training the hyperparameters by max-

imising the likelihood function, and then one can obtain the joint normal distribution over functions without assuming any specific model.

We use the squared exponential function, which is the most general form of covariance function, as the kernel function to acquire the $H(z)$ and $H'(z)$, namely

$$k(x, x') = \sigma_f^2 e^{-\frac{(x-x')^2}{2l^2}}, \quad (\text{A1})$$

where the σ_f and l are the hyperparameters. Starting from the data-driven reconstructed $w(z)$ we obtain the $H(z)$ and $H'(z)$ functions by GAPP (Gaussian Processes in Python), and then the $f(T)$ function presented in Fig. 5. Note that the Gaussian processes method pays more attention to the overall distribution, and therefore the correlation between each $H(z)$ and $H'(z)$ samples will be reduced. This will lead to larger errors in the reconstruction results at high redshift.

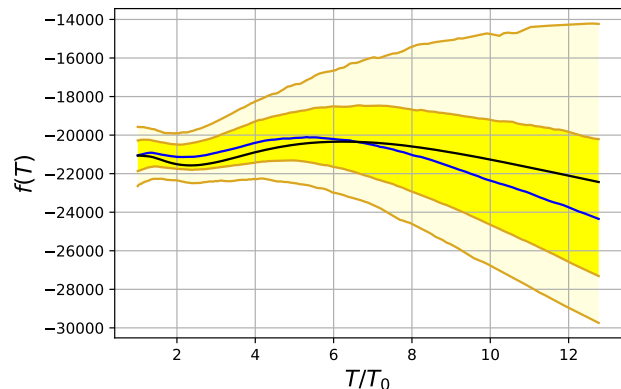


FIG. 5. The reconstructed $f(T)$ form, arising through Gaussian processes. The yellow and light yellow regions mark the 1σ and 2σ confidence level respectively, the blue curve represents the reconstructed mean values, and the black curve arises using the best-fit curve of $H(z)$ and $H'(z)$ obtained by GAPP. Note the larger errors at high redshift comparing to Fig. 4 due to the reduced correlation between each $H(z)$ and $H'(z)$ samples (see text).

-
- [1] A. G. Riess *et al.* (Supernova Search Team), *Astron. J.* **116**, 1009 (1998), [arXiv:astro-ph/9805201](#).
 - [2] S. Perlmutter *et al.* (Supernova Cosmology Project), *Astrophys. J.* **517**, 565 (1999), [arXiv:astro-ph/9812133](#).
 - [3] A. G. Riess, S. Casertano, W. Yuan, L. M. Macri, and D. Scolnic, *Astrophys. J.* **876**, 85 (2019), [arXiv:1903.07603 \[astro-ph.CO\]](#).
 - [4] Y. Akrami *et al.* (Planck), (2018), [arXiv:1807.06205 \[astro-ph.CO\]](#).
 - [5] N. Aghanim *et al.* (Planck), (2018), [arXiv:1807.06209 \[astro-ph.CO\]](#).
 - [6] T. Delubac *et al.* (BOSS), *Astron. Astrophys.* **574**, A59 (2015), [arXiv:1404.1801 \[astro-ph.CO\]](#).
 - [7] L. Kazantzidis and L. Perivolaropoulos, *Phys. Rev. D* **97**, 103503 (2018), [arXiv:1803.01337 \[astro-ph.CO\]](#).
 - [8] G. Lambiase, S. Mohanty, A. Narang, and P. Parashari, *Eur. Phys. J. C* **79**, 141 (2019), [arXiv:1804.07154 \[astro-ph.CO\]](#).
 - [9] E. Di Valentino *et al.*, (2020), [arXiv:2008.11284 \[astro-ph.CO\]](#).
 - [10] S. Tsujikawa, *Class. Quant. Grav.* **30**, 214003 (2013), [arXiv:1304.1961 \[gr-qc\]](#).
 - [11] R. Caldwell, *Phys. Lett. B* **545**, 23 (2002), [arXiv:astro-ph/9908168](#).
 - [12] S. M. Carroll, M. Hoffman, and M. Trodden, *Phys. Rev. D* **68**, 023509 (2003), [arXiv:astro-ph/0301273](#).

- [13] Y.-F. Cai, E. N. Saridakis, M. R. Setare, and J.-Q. Xia, *Phys. Rept.* **493**, 1 (2010), arXiv:0909.2776 [hep-th].
- [14] T. P. Sotiriou and V. Faraoni, *Rev. Mod. Phys.* **82**, 451 (2010), arXiv:0805.1726 [gr-qc].
- [15] Y.-F. Cai, S. Capozziello, M. De Laurentis, and E. N. Saridakis, *Rept. Prog. Phys.* **79**, 106901 (2016), arXiv:1511.07586 [gr-qc].
- [16] S. Capozziello and M. De Laurentis, *Phys. Rept.* **509**, 167 (2011), arXiv:1108.6266 [gr-qc].
- [17] S. Capozziello, R. D'Agostino, and O. Luongo, *Gen. Rel. Grav.* **49**, 141 (2017), arXiv:1706.02962 [gr-qc].
- [18] J.-P. Dai, Y. Yang, and J.-Q. Xia, *Astrophys. J.* **857**, 9 (2018).
- [19] G. Arciniega, M. Jaber, L. G. Jaime, and O. A. Rodríguez-López, (2021), arXiv:2102.08561 [astro-ph.CO].
- [20] G.-B. Zhao *et al.*, *Nature Astron.* **1**, 627 (2017), arXiv:1701.08165 [astro-ph.CO].
- [21] Y. Wang, L. Pogosian, G.-B. Zhao, and A. Zucca, *Astrophys. J. Lett.* **869**, L8 (2018), arXiv:1807.03772 [astro-ph.CO].
- [22] S. Capozziello, Ruchika, and A. A. Sen, *Mon. Not. Roy. Astron. Soc.* **484**, 4484 (2019), arXiv:1806.03943 [astro-ph.CO].
- [23] E. Di Valentino, A. Melchiorri, and J. Silk, *Phys. Lett. B* **761**, 242 (2016), arXiv:1606.00634 [astro-ph.CO].
- [24] E. Di Valentino, A. Melchiorri, E. V. Linder, and J. Silk, *Phys. Rev. D* **96**, 023523 (2017), arXiv:1704.00762 [astro-ph.CO].
- [25] S. Vagnozzi, *Phys. Rev. D* **102**, 023518 (2020), arXiv:1907.07569 [astro-ph.CO].
- [26] L. Visinelli, S. Vagnozzi, and U. Danielsson, *Symmetry* **11**, 1035 (2019), arXiv:1907.07953 [astro-ph.CO].
- [27] Y.-F. Cai and E. N. Saridakis, *J. Cosmol.* **17**, 7238 (2011), arXiv:1108.6052 [gr-qc].
- [28] S.-F. Yan, P. Zhang, J.-W. Chen, X.-Z. Zhang, Y.-F. Cai, and E. N. Saridakis, *Phys. Rev. D* **101**, 121301 (2020), arXiv:1909.06388 [astro-ph.CO].
- [29] C. Li, Y. Cai, Y.-F. Cai, and E. N. Saridakis, *JCAP* **10**, 001 (2018), arXiv:1803.09818 [gr-qc].
- [30] S. Nesseris, S. Basilakos, E. N. Saridakis, and L. Perivolaropoulos, *Phys. Rev. D* **88**, 103010 (2013), arXiv:1308.6142 [astro-ph.CO].
- [31] S. Basilakos, S. Nesseris, F. K. Anagnostopoulos, and E. N. Saridakis, *JCAP* **08**, 008 (2018), arXiv:1803.09278 [astro-ph.CO].
- [32] B. Xu, H. Yu, and P. Wu, *Astrophys. J.* **855**, 89 (2018).
- [33] F. K. Anagnostopoulos, S. Basilakos, and E. N. Saridakis, *Phys. Rev. D* **100**, 083517 (2019), arXiv:1907.07533 [astro-ph.CO].
- [34] J. Levi Said, J. Mifsud, D. Parkinson, E. N. Saridakis, J. Sultana, and K. Z. Adami, *JCAP* **11**, 047 (2020), arXiv:2005.05368 [astro-ph.CO].
- [35] M. Krššák and E. N. Saridakis, *Class. Quant. Grav.* **33**, 115009 (2016), arXiv:1510.08432 [gr-qc].
- [36] M. Krssak, R. van den Hoogen, J. Pereira, C. Böhmer, and A. Coley, *Class. Quant. Grav.* **36**, 183001 (2019), arXiv:1810.12932 [gr-qc].
- [37] V. De Andrade, L. Guillen, and J. Pereira, in *9th Marcel Grossmann Meeting on Recent Developments in Theoretical and Experimental General Relativity, Gravitation and Relativistic Field Theories (MG 9)* (2000) arXiv:gr-qc/0011087.
- [38] A. Unzicker and T. Case, (2005), arXiv:physics/0503046.
- [39] R. Aldrovandi and J. G. Pereira, *Teleparallel Gravity: An Introduction*, Vol. 173 (Springer, 2013).
- [40] Y.-F. Cai, M. Khurshudyan, and E. N. Saridakis, *Astrophys. J.* **888**, 62 (2020), arXiv:1907.10813 [astro-ph.CO].
- [41] M.-J. Zhang and J.-Q. Xia, *JCAP* **12**, 005 (2016), arXiv:1606.04398 [astro-ph.CO].
- [42] R. Briffa, S. Capozziello, J. Levi Said, J. Mifsud, and E. N. Saridakis, *Class. Quant. Grav.* **38**, 055007 (2020), arXiv:2009.14582 [gr-qc].
- [43] P. A. R. Ade *et al.* (Planck), *Astron. Astrophys.* **594**, A13 (2016), arXiv:1502.01589 [astro-ph.CO].
- [44] M. Betoule *et al.* (SDSS), *Astron. Astrophys.* **568**, A22 (2014), arXiv:1401.4064 [astro-ph.CO].
- [45] F. Beutler, C. Blake, M. Colless, D. H. Jones, L. Staveley-Smith, L. Campbell, Q. Parker, W. Saunders, and F. Watson, *Mon. Not. Roy. Astron. Soc.* **416**, 3017 (2011), arXiv:1106.3366 [astro-ph.CO].
- [46] A. J. Ross, L. Samushia, C. Howlett, W. J. Percival, A. Burden, and M. Manera, *Mon. Not. Roy. Astron. Soc.* **449**, 835 (2015), arXiv:1409.3242 [astro-ph.CO].
- [47] D. Parkinson *et al.*, *Phys. Rev. D* **86**, 103518 (2012), arXiv:1210.2130 [astro-ph.CO].
- [48] C. Heymans *et al.*, *Mon. Not. Roy. Astron. Soc.* **432**, 2433 (2013), arXiv:1303.1808 [astro-ph.CO].
- [49] A. G. Riess *et al.*, *Astrophys. J.* **826**, 56 (2016), arXiv:1604.01424 [astro-ph.CO].
- [50] M. Moresco, L. Pozzetti, A. Cimatti, R. Jimenez, C. Maraston, L. Verde, D. Thomas, A. Citro, R. Tojeiro, and D. Wilkinson, *JCAP* **05**, 014 (2016), arXiv:1601.01701 [astro-ph.CO].
- [51] G.-B. Zhao *et al.* (BOSS), *Mon. Not. Roy. Astron. Soc.* **466**, 762 (2017), arXiv:1607.03153 [astro-ph.CO].
- [52] D. Huterer and G. Starkman, *Phys. Rev. Lett.* **90**, 031301 (2003), arXiv:astro-ph/0207517.
- [53] T. Holsclaw, U. Alam, B. Sanso, H. Lee, K. Heitmann, S. Habib, and D. Higdon, *Phys. Rev. Lett.* **105**, 241302 (2010), arXiv:1011.3079 [astro-ph.CO].
- [54] M. Seikel, C. Clarkson, and M. Smith, *JCAP* **06**, 036 (2012), arXiv:1204.2832 [astro-ph.CO].
- [55] S. Dodelson, M. Kaplinghat, and E. Stewart, *Phys. Rev. Lett.* **85**, 5276 (2000), arXiv:astro-ph/0002360.
- [56] B. Feng, M. Li, Y.-S. Piao, and X. Zhang, *Phys. Lett. B* **634**, 101 (2006), arXiv:astro-ph/0407432.
- [57] R. Lazkoz, V. Salzano, and I. Sendra, *Phys. Lett. B* **694**, 198 (2011), arXiv:1003.6084 [astro-ph.CO].
- [58] J.-Z. Ma and X. Zhang, *Phys. Lett. B* **699**, 233 (2011), arXiv:1102.2671 [astro-ph.CO].
- [59] F. Pace, C. Fedeli, L. Moscardini, and M. Bartelmann, *Mon. Not. Roy. Astron. Soc.* **422**, 1186 (2012), arXiv:1111.1556 [astro-ph.CO].
- [60] S. Pan, E. N. Saridakis, and W. Yang, *Phys. Rev. D* **98**, 063510 (2018), arXiv:1712.05746 [astro-ph.CO].